IIETA International Information and Engineering Technology Association
Advancing the World of Information and Engineering

Instrumentation Mesure Métrologie
Vol. 24, No. 1, February, 2025, pp. 89-95
Journal homepage: http://iieta.org/journals/i2m

Enhanced Optical and Structural Properties of ZnO NPs Doped PVA/PEG/PVP and its Use in Bacterial Activity

Huda M. Al-asadi [1*], Saba A. Obaid[2], Rusul A. Ghazi[2]

[1] Ministry of Education, Baghdad 10065, Iraq
[2] Physics Department, Science College, University of Babylon, Hilla 51001, Iraq

Corresponding Author Email: hudaalasadi2014@gmail.com

https://doi.org/10.18280/i2m.240110

Received: 28 September 2024
Revised: 12 February 2025
Accepted: 19 February 2025
Available online: 28 February 2025

Keywords:
optical features, antibacterial activity, X-ray diffraction, polyvinyl alcohol, polyethene glycol, polyvinyl-Pyrrolidone, ZnO nanoparticles

ABSTRACT

Current study combined zinc oxide nanoparticles (Nano-ZnO) with a polymer mixture to improve their optical, structural, and antibacterial efficacy along with maintaining biocompatibility and sustainability. Nano-ZnO might be uniquely added to the polymer mix to enhance the blend's physical and antibacterial properties. Nanomaterials (NCs) during the loading procedure, three distinct Nano-ZnO concentrations were enclosed in polyvinyl pyrrolidone (PVP), polyethylene glycol (PEG), and polyvinyl alcohol (PVA). Doping improved the optical characteristics; there was a drop in the forbidden indirect photonic energy gap from 4.9 to 4 eV and a decrease in the allowed indirect photonic energy gap from 5 to 4 eV. Utilizing X-ray diffraction (XRD), scanning electron microscopy (SEM), and UV visible, the produced films were examined. According to the SEM pictures, the Nano-ZnO were evenly distributed throughout the polymer mixture, with a few weak aggregation.

1. INTRODUCTION

The research issue revolves around the necessity to create nanocomposite materials that include ZnO nanoparticles, while ensuring a balance between optical, textural, and antibacterial characteristics, along with maintaining biocompatibility and sustainability. Recent developments in the biomedical and pharmaceutical areas have been greatly aided by creating adaptable biomaterials that may be custom-made to satisfy even the most demanding needs [1]. These biomaterials have been made with great control, starting with the polymer synthesis stage and continuing through the materials production and final property design stages [2, 3].

Among the most often utilized polymers in the biological sciences is PVA. Moreover, PVA offers three interesting properties for a polymer meant to be utilized as a delivery system: low protein adsorption, strong surface stability, and low chelation, hence lowering cell adherence in contrast to other hydrogels [4, 5]. Because of all the previously mentioned properties, PVA is projected to be extensively used in many biomedical applications, including wound bandages [6].

Since its discovery, Polyvinylpyrrolidone (PVP) has been a popular polymer with many interesting characteristics. Among the remarkable physical and chemical properties that make it fit as a biomaterial in many critical medical and nonmedical applications (inks, coatings, paper, ceramics, adhesives, membranes, electrical and optical uses, medicine and pharmaceutical industry, textiles and fibres, photography and lithography, institutional and industrial and home), are chemical stability, nontoxicity, biocompatibility, good solubility in water and many organic solvents, and affinity to complex hydrophobic and hydrophilic substances [7-10].

PVA, PVP, and PVA/PVP-based biomaterials have a well-documented history in various commercial, industrial, food, pharmaceutical, biotechnological advanced biomedical, and utilizations. These applications are attributed to their high mechanical characteristics, strong biocompatibility, and biodegradability [11].

The most biocompatible synthetic polymer substance is polyethene glycol. Its uses in medical devices are constantly being explored, in addition to their widespread usage in medicine for long-term and synergistic benefits. Polyethene glycol material can be widely used in various surgical operations equipment materials for anti-adhesion, anti-leakage, hemostasis treatment, and adhesion of wounds because of its advantages of low immunogenicity, nontoxicity, good biocompatibility, and solubility [12-14].

Nanomaterials have drawn more attention recently because of their special qualities, which make them attractive for a range of industrial and medicinal uses. Because of their remarkable physical and chemical features, such as their antibacterial activity, high thermal stability, and unique optical and electrical qualities, zinc oxide nanoparticles (ZnO NPs) stand out among these materials [15, 16]. The low toxicity and biodegradability of ZnO nanoparticles is its essential characteristics. For adults, zinc dioxide ($Zn2+$) is an essential trace element that plays several roles in metabolism (a daily intake of around 10 mg is advised), The developed nanocomposite materials containing ZnO NPs can significantly enhance product performance across various fields, including Biomedical Applications: These materials

can be used in antibacterial coatings for sterilization applications, wound dressings, and medical devices, such as smart band [17-24].

2. EXPERIMENTAL WORK

This work uses Nano zinc oxide particles as filler and polyvinyl pyrrolidone (PVP), polyethene glycol (PEG), and polyvinyl alcohol (PVA) as a matrix. Distillation water was used to dissolve the polyvinyl alcohol, polyethene glycol, and polyvinyl pyrrolidone (50 weight per cent polyvinyl alcohol, 25 weight per cent polyethene glycol, and 25 weight per cent polyvinyl pyrrolidone). In the polymer matrix, the Nano Zinc oxide was added in different weight percentages: 0, 0.02, 0.04, and 0.06 as shown in Table 1. The nanocomposites were prepared using the casting procedure. We used Zinc nanoparticles with a particle size of 20 nanometers and a purity of 99.9 from SAT Nano Technology Material Co., Ltd.

Table 1. PVA/PEG/PVP/ZnO weight percentages

PVA (gm)	PEG (gm)	PVP (gm)	ZnO (gm)
0.5	0.25	0.25	------
0.6	0.2	0.2	0.02
0.7	0.15	0.15	0.04
0.8	0.1	0.1	0.06

The absorbance for nanocomposites was calculated using a spectrum measuring device of the Double-Beam Spectrophotometer (UV-1800) type produced by the Shimadzu company in Japan, with a wavelength range of 190 to 1100 nm. The Pert High Score (2008) X-ray diffractometer examined the crystal structure.

3. RESULTS AND DISCUSSIONS

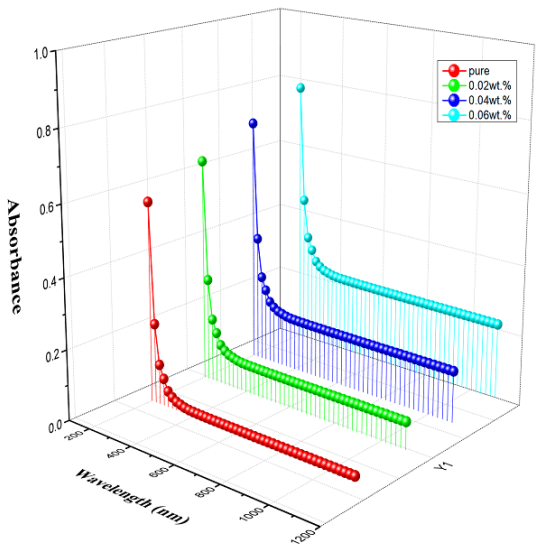

Figure 1. The absorbance as a wavelength function of (PVA/PEG/PVP/ZnO) nanocomposites

The PVA/PEG/PVP blend's optical characteristics and those of its additives with (0, 0.02,0.04, and 0.06) wt.% from ZnO nanoparticles were investigated in the wavelength range of 190–1100 nm. The PVA/PEG/PVP polymer blend's absorption spectra both before and after adding ZnO NPs were shown concerning wavelengths. Figure 1 shows that the low magnitudes in the visible and near-infrared regions of this absorbance spectrum are caused by the insufficient energy of the incoming photons to interact with and transmit atoms at a high wavelength. The absorbance rose at low wavelength magnitudes because of an interaction between the incoming photon and the mix. The optical absorbance spectrum was improved by loading ZnO NPs into the polymeric blend; this may have been caused by the uniform dispersion of ZnO NPs inside the polymer blends.

With an increase in wavelength, there is a decline in absorbance, a typical behavior for nanomaterials such as ZnO that possess a significant bandgap. Higher absorption is observed at shorter wavelengths within the UV spectrum, while absorption in the visible range diminishes progressively. When high-energy photons are absorbed, ZnO affects electronic transitions, exciting electrons from the valence band into the conduction band.

As the wavelength increased, the coefficient of absorption (α) magnitudes fell for produced films. The NCs (α) were determined using [25]:

$$\alpha = 2.303(A/t) \quad (1)$$

As seen in Figure 2, the magnitudes of (α) rose when ZnO NPs increased. Since the coefficient of absorption magnitudes were less than 10^4 $cm^{-1,}$ the possibility of indirect transitions increased.

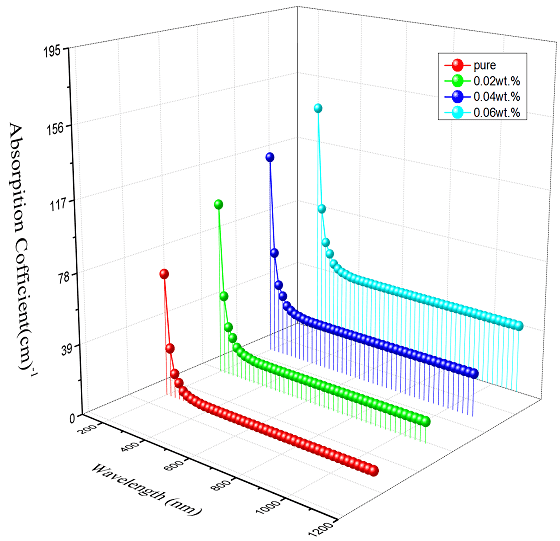

Figure 2. The coefficient of absorption α(cm)-1 as a wavelength function (nm) for (PVA/PEG/PVP/ZnO) nanocomposites

The nanocomposite's extinction of absorption (k) has been calculated using [26]:

$$k = \alpha\lambda/4\pi \quad (2)$$

For prepared films, (k) increases as the ZnO NP concentration rises. Figure 3 illustrates the (k) of PVA/PEG/PVP with varying ZnO NP weight percentages.

The T_{auc} model [27, 28] has been utilized to determine the direct and indirect optical energy gap of the (PVA/PEG/PVP/ZnO) nanocomposites films:

$$\alpha h\upsilon = B\,(h\upsilon - E_g^{\,opt.} \pm E_{ph.})^r \quad (3)$$

where, $E_{ph.}$: phonon energy, is (-) once phonon absorption, and (+) once phonon emission.

(r = 2) for the indirect allowed transition.
(r = 3) for the indirect forbidden transition.

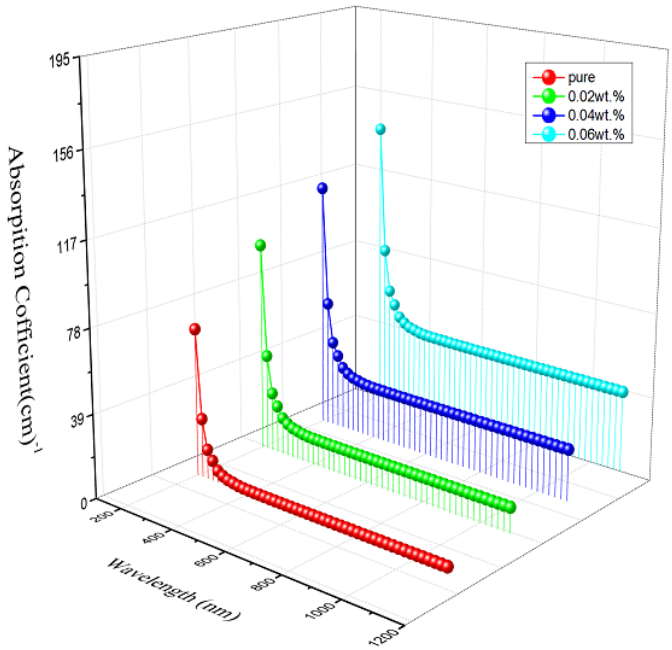

Figure 3. The Extinction of absorption as a wavelength function for (PVA/PEG/PVP/ZnO) nanocomposites

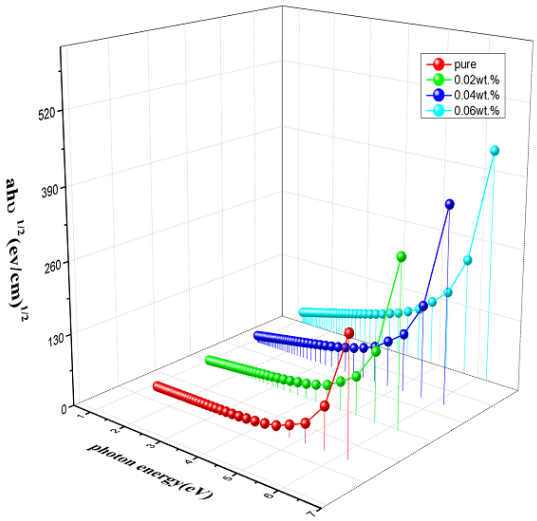

Figure 4. The energy gap for the indirect allowed transition $(\alpha h\upsilon)^{1/2}$ as a photon energy function of (PVA/PEG/PVP/ZnO) nanocomposites

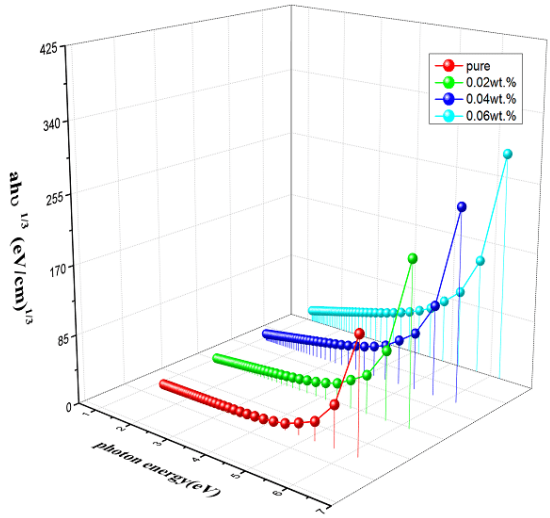

Figure 5. The energy gap for the indirect forbidden transition$(\alpha h\upsilon)^{1/3}$ as a photon energy function of (PVA/PEG/PVP/ZnO) nanocomposites

Figure 4 and Figure 5 present the allowed and forbidden indirect optical energy gaps. Eg is represented by the straight-line extrapolation of photon energy at zero $(\alpha h\nu)^{1/2}$ and $(\alpha h\nu)^{1/3}$, respectively. The fact that the energy gap magnitudes decrease as ZnO NP concentration increases shows that the films were semiconductors. An important feature that can impact a variety of applications, particularly in photocatalysis, optoelectronics, sensors, and transparent conductive films, is the decrease in the optical energy band gap with increasing ZnO nanoparticle (ZnO NP) concentration.

Antibacterial tests

Bacterial suspensions of Acinetobacter baumannii and E. coli to a final concentration of 1.5×10^8 CFU/mL. Suspensions were adjusted to a 0.5 McFarland standard and standardized with physiological saline. A sterile cotton swab was used to distribute the bacterial inoculum uniformly throughout the Mueller-Hinton agar plates. To be evaluated, test samples were placed on an agar surface. For a full day, the plates were incubated at 37°C. Following incubation, the inhibition zones surrounding the loaded samples were examined to determine the antibacterial activity.

For determining the (PVA/PEG/PVP/ZnO) NCs Antibacterial tests, sample organisms consisting of Gram-negative (G−) bacterial offspring involving E. coli (E.c) and Acinetobacter baumanii (AB), as well as Gram-positive (G+) species like Staphylococcus aureus (S.a) and Streptococcus pyrogens (SP). In 5 mm of DMSO soup, the bacterial kinetics of (PVA/PEG/PVP/ZnO) NCs were seen to develop with different doping of ZnO NPs. The outcomes demonstrated the nanocomposite's (PVA/PEG/PVP/ZnO) definite inhibitory

action against the two varieties of positive bacteria. Following a 24-hour incubation period at 37 degrees, a variation was noted in the impact of varying nanocomposite concentrations on the inhibition of individual positive bacterial species. The effects of the nanocomposite ranged from 6 to 20 mm in inhibition diameters, as Table 2 illustrates. The results also demonstrate an increase in inhibition diameters with increasing nanoparticle addition for both Streptococcus pyogenes (SP) and Staphylococcus aureus (S.a.), as seen in Figures 6, 7 and 8.

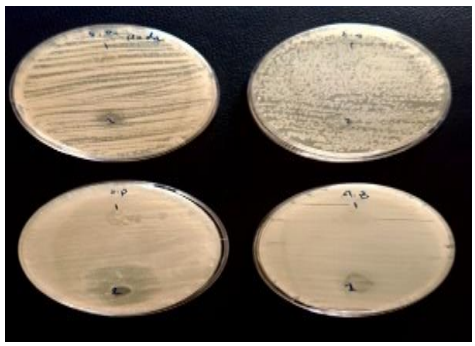

Figure 6. Antibacterial activity of (PVA/ PEG /PVP/ZnO) nanocomposites for pure and 0.02 wt.% against various pathogenetic bacterial strains

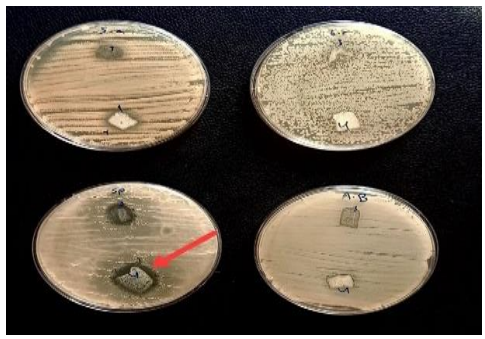

Figure 7. Antibacterial activity of (PVA/ PEG /PVP/ZnO) nanocomposites for 0.04 and 0.06 wt.% against various pathogenetic bacterial strains

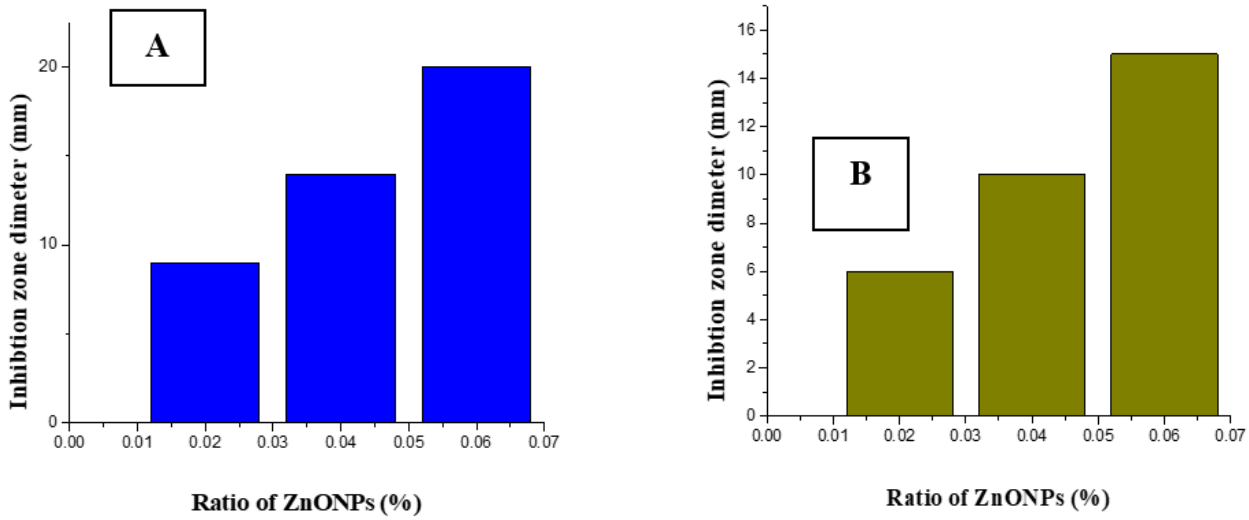

Figure 8. The inhibition zone diameter of (A) S. pyogens, (B) S. aureus vs. NPs-ZnO doped PVA/PEG/PVP weight percentage

Table 2. The inhibition zone diameter of E. coli (E.c), Acinetobacter baumanii (AB), Staphylococcus aureus (S.a) and Streptococcus pyrogens (SP), ZnO NPs doped PVA/PEG/PVP weight percentage

S. aureus	S. pyrogens	E. coli	A. baumanii	Substrate Concentrations
----	----	----	----	Pure
6	9	----	----	0.02
10	14	----	----	0.04
15	20	----	----	0.06

Table 3. Experimental XRD data for (PVA/PEG/PVP/ZnO) nanocomposites

Average G.S (nm)	Dislocation Density (δ)	G.S (nm)	Average FWHM (rad)	FWHM (rad)	dhkl Exp (A^O)	2Θ (Deg.)	(hkl)	Substrate Concentration
5.56	1.79E-03	2.36	2.20	3.4188	4.3	20.49	(100)	pure
	1.30E-04	8.76		0.984	1.99	45.809	(201)	
36.5	3.20E-04	5.59	0.91	1.44	4.663	19.0	(100)	0.02%
	2.11E-04	6.89		1.20	2.7965	32.0	(200)	
	1.06E-06	97.1		0.09	1.845	49.3	(024)	
42.4	1.25E-06	89.6	0.78	0.09	4.464	19.9	(100)	0.04%
	3.15E-04	5.64		1.44	3.750	23.7	(012)	
	1.21E-06	90.9		0.09	3.229	27.6	(111)	
	1.35E-04	8.61		0.96	2.782	32.1	(200)	
	1.17E-06	92.5		0.09	2.567	34.9	(110)	
	1.32E-04	8.72		0.96	2.444	36.7	(110)	
	3.69E-04	5.20		1.68	1.844	49.4	(024)	

	1.13E-04	9.42		0.96	1.61	57.1	(122)	
	2.38E-04	6.49		1.44	1.456	63.4	(300)	
	8.74E-07	107		0.09	1.364	68.8	(208)	
	0.000503	4.458321		1.808	4.549	19.494	(100)	
	5.62E-06	42.16889		0.196	2.791	32.032	(200)	
	1.17E-06	92.53167		0.09	2.567	34.914	(110)	
	0.000132	8.714155		0.96	2.458	36.522	(110)	
	3.21E-05	17.66248		0.492	1.9	47.817	(018)	
45.67	4.27E-05	15.30819	0.602	0.5904	1.61	56.958	(211)	0.06%
	0.000238	6.479953		1.44	1.468	63.277	(125)	
	5.25E-05	13.80567		0.6888	1.401	66.681	(300)	
	5.13E-05	13.9656		0.6888	1.366	68.65	(301)	
	8.65E-07	107.4955		0.09	1.3667	69.6	(400)	
	8E-07	111.8303		0.09	1.25	75.756	(331)	
	7.74E-07	113.6383		0.09	1.223	78.07	(420)	

Meanwhile, nanocomposites did not significantly inhibit Acinetobacter baumanii (AB) and E. coli (E.c.) negative bacteria at any dose. The bacterial cell wall's structure affects the ZnO nanoparticles' antibacterial action. Gram-positive bacteria possess a thick cell wall comprising many peptidoglycan layers; in contrast, the cell wall of Gram-negative bacteria is complicated. The outside packs a thin layer of peptidoglycan membrane. For bacteria that are Gram-positive, ZnO nanoparticles engage with the cell wall's outer layers, which have many pores, making it an easy path for the Zinc oxide nanoparticles to enter cells and promote the leaking of the internal components, ultimately leading to the demise of the cell [28-32]

SEM images

As seen in Figure 9, the SEM was also used to examine the morphology and surface fraction of the NCs films. An SEM picture of a uniformly morphological, homogenous polymer surface is shown in Figure 9 (A). Zinc oxide nanoparticles caused the surface's composition to shift. As seen in Figure 9 (B, C, and D), this would suggest a homogenous development process free from aggregations. ZnO NPs' size on NC surfaces was assessed using SEM images. Nano-ZnO particle sizes varied within a 500-nanometer range.

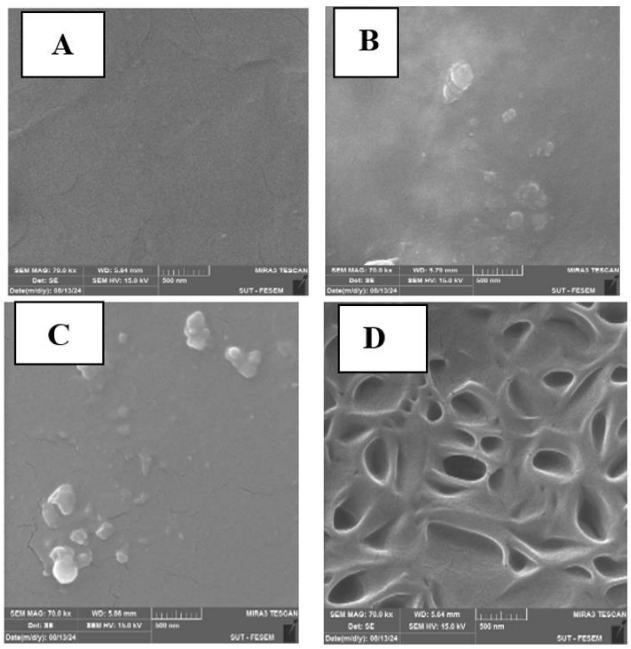

Figure 9. SEM photomicrographs for (PVA/ PEG /PVP/ZnO) nanocomposites (A) for pure, (B) 0.02wt.%, (C) for 0.04wt.%, (D) for 0.06wt.%

X-ray diffraction (XRD)

Figure 10 presents the XRD peaks of the PVA/PEG/PVP polymer mix with and without varying ZnO NPs contents. Two peaks on the PVA/PEG/PVP XRD chart ($2\theta = 20.49°$ and $2\theta = 45.809°$) show the polymer blend's semi-crystalline character.

Using the information from the obtained diffraction pattern, we can calculate the average grain size using Scherer's equation and the rate at which the crystals grew inside the crystal lattice. Next, we can calculate the exposure amount for the characteristic peaks (β), which depends on the width of the middle of the peak (FWHM), which is measured in radial units (rad). Finally, the granular size is calculated using Eq. (4) [33]:

$$GS = (0.94\ \lambda) / \beta_{FWHM.\cos}\theta \quad (4)$$

The sharpness of the PVA/PEG/PVP peak increased with ZnO NPs, which may result from their interactions. The XRD peaks indicate that doping improved the polymer blend's crystallinity. The PVA/PEG/PVP doped with ZnO NPs exhibits a cubic structure. We notice an increase in the grain size measurement with the increase of added ZnO NPs, which matches the results of the SEM photomicrographs. The experimental XRD data for (PVA/PEG/PVP/ZnO) nanocomposites shown in Table 3.

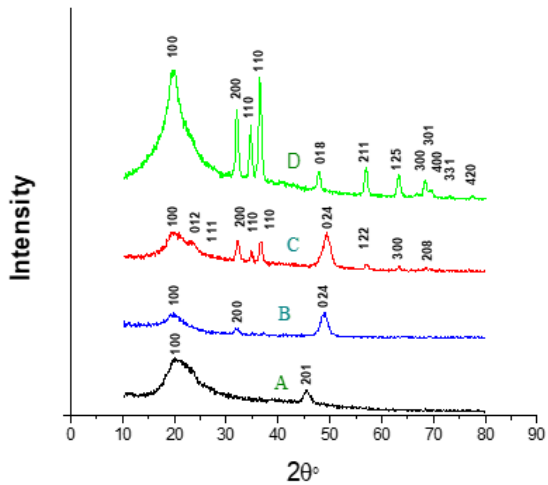

Figure 10. XRD for (PVA/ PEG /PVP/ZnO) nanocomposites (A) for pure, (B) 0.02wt.%, (C) for 0.04wt.%, (D) for 0.06wt.%

4. Conclusions

The casting approach effectively created the

PVA/PEG/PVP polymer mix with and without ZnO NPs. As ZnO NP concentration rose, so did the optical and extinction of absorptions, while the optical energy gap decreased. There was a drop in the forbidden indirect photonic energy gap from 4.9 to 4 eV and a decrease in the allowed indirect photonic energy gap from 5 to 4 eV. Following loading, there was a significant increase in the inhibitory zone diameters of Streptococcus pyogens (SP) and Staphylococcus aureus (S.a.). The ZnO NPs were effectively dispersed throughout the mix with a few faint agglomerations. They increased the grain size measurement with added ZnO NPs according to the SEM pictures and XRD. The peaks of XRD emerged as the blend's semi-crystalline structure.

ZnO nanoparticles that are evenly distributed throughout a matrix may sustain a large surface area, which improves light absorption and scattering and results in better optical characteristics including UV absorption and photoluminescence, and more surface area is available for contact with bacterial cells when ZnO nanoparticles are scattered evenly. Better antibacterial action is made possible by the particles' increased ability to pass through cell membranes.

The surface modification of the nanoparticles or optimization of the blending process might be altered to further enhance dispersion and lessen aggregation.

ACKNOWLEDGMENT

The authors would like to thank head of the physics department - College of Babylon University, to do the practicle part in the department laboratories.

REFERENCES

[1] Sallal, H.A., Mahboba, M.H., Radhi, M.S., Hanif, A., Al-Khafaji, Z.S., Ahmad, S., Yaseen, Z.M. (2024). Effect of adding (ZrO2-ZnO) nanopowder on the polymer blend (lamination and methyl vinyl silicone) in a hybrid nanocomposite material. Journal of King Saud University-Science, 36(2): 103061.

[2] Knop, K., Hoogenboom, R., Fischer, D., Schubert, U.S. (2010). Poly(ethylene glycol) in drug delivery: Pros and cons as well as potential alternatives. Angewandte Chemie International Edition, 49(36): 6288-6308. https://doi.org/10.1002/anie.200902672

[3] Xu, M.S, Iwai, H., Mei, Q.S., Fujita, D., Su, H.X., Chen, H.Z., Hanagata, N. (2012). Formation of nano-bio-complex as nanomaterials dispersed in a biological solution for understanding nanobiological interactions. Scientific Reports, 2: 1-6. https://doi.org/10.1038/srep00406

[4] Rivera-Hernández, G., Antunes-Ricardo, M., Martínez-Morales, P., Sánchez, M.L. (2021). Polyvinyl alcohol based-drug delivery systems for cancer treatment. International Journal of Pharmaceutics, 600: 120478. https://doi.org/10.1016/j.ijpharm.2021.120478

[5] Gajra, B., Pandya, S.S., Vidyasagar, G., Rabari, H., Dedania, R.R., Rao, S. (2012). Poly vinyl alcohol hydrogel and its pharmaceutical and biomedical applications: A review. International Journal of Pharmaceutical Research, 4(2): 20-26.

[6] Muppalaneni S, Omidian H. (2013). Polyvinyl alcohol in medicine and pharmacy: A perspective. Journal of Developing Drugs, 2(3): 1-5.

[7] Franco, P., De Marco, I. (2020). The use of poly (N-vinyl pyrrolidone) in the delivery of drugs: A review. Polymers, 12(5): 1114. https://doi.org/10.3390/polym12051114

[8] Hu M, Li C, Li X, Zhou, M., Sun, J., et al. (2018). Zinc oxide/silver bimetallic nanoencapsulated in PVP/PCL nanofibres for improved antibacterial activity[J]. Artificial cells, nanomedicine, and biotechnology, 46(6): 1248-1257. https://doi.org/10.1080/21691401.2017.1366339

[9] Frauenfelder, L.J. (1974). Universal chromatographic-colorimetric method for the determination of trace amounts of polyvinylpyrrolidone and its copolymers in foods, beverages, laundry products, and cosmetics. Journal of AOAC International, 57(4): 796-800. https://doi.org/10.1093/jaoac/57.4.796

[10] Teodorescu, M., Bercea, M. (2015). Poly(vinylpyrrolidone) – A versatile polymer for biomedical and beyond medical applications. Polymer-Plastics Technology and Engineering, 54(9): 923-943. https://doi.org/10.1080/03602559.2014.979506

[11] Teodorescu, M., Bercea, M., Morariu, S. (2019). Biomaterials of PVA and PVP in medical and pharmaceutical applications: Perspectives and challenges. Biotechnology Advances, 37(1): 109-131. https://doi.org/10.1016/j.biotechadv.2018.11.008

[12] D'souza, A.A., Shegokar, R. (2016). Polyethylene glycol (PEG): A versatile polymer for pharmaceutical applications. Expert Opinion on Drug Delivery, 13(9): 1257-1275. https://doi.org/10.1080/17425247.2016.1182485

[13] Nugraha, B. (2016). Application of PEG in drug delivery system. In Gels Handbook: Fundamentals, Properties, and Applications , pp. 137-147. https://doi.org/10.1142/9789813140417_0006

[14] Jeon, O., Samorezov, J.E., Alsberg, E. (2014). Single and dual crosslinked oxidized methacrylated alginate/PEG hydrogels for bioadhesive applications. Acta Biomaterialia, 10(1): 47-55. https://doi.org/10.1016/j.actbio.2013.09.004

[15] Hutanu, D. (2014). Recent applications of polyethylene glycols (PEGs) and PEG derivatives. Modern Chemistry & Applications, 2(2). https://doi.org/10.4172/2329-6798.1000132

[16] Zhang, Z.Y., Xiong, H.M. (2015). Photoluminescent ZnO nanoparticles and their biological applications. Materials, 8(6): 3101-3127. https://doi.org/10.3390/ma8063101

[17] Kielbik, P., Kaszewski, J., Rosowska, J., Wolska, E., Witkowski, B.S. et al. (2017). Biodegradation of the ZnO:Eu nanoparticles in the tissues of adult mouse after alimentary application. Nanomedicine: Nanotechnology, Biology, and Medicine, 13(3): 843-852. https://doi.org/10.1016/j.nano.2016.11.002

[18] Raguvaran, R., Manuja, B.K., Chopra, M., Thakur, R., Anand, T., Kalia, A., Manuja, A. (2017). Sodium alginate and gum acacia hydrogels of ZnO nanoparticles show wound healing effect on fibroblast cells. International Journal of Biological Macromolecules, 96: 185-191. https://doi.org/10.1016/j.ijbiomac.2016.12.009

[19] Jones, N., Ray, B., Ranjit, K.T., Manna, A.C. (2008). Antibacterial activity of ZnO nanoparticle suspensions

on a broad spectrum of microorganisms. FEMS Microbiology Letters, 279(1): 71-76. https://doi.org/10.1111/j.1574-6968.2007.01012.x
[20] Morkoç, H., Özgür, Ü. (2009). General properties of ZnO. In Zinc Oxide: Fundamentals, Materials and Device Technology, pp. 1-76. https://doi.org/10.1002/9783527623945.ch1
[21] Sulaiman, R., Ghaffar, A., Perveen, S., Ashraf, D., Tariq, I., Shakir, T. (2023). Synthesis, characterization, and biomedical applications of zinc oxide nanoparticles. BME Horizon, 1(3).
[22] Sawai, J. (2003). Quantitative evaluation of antibacterial activities of metallic oxide powders (ZnO, MgO, and CaO) by conductimetric assay. Journal of Microbiological Methods, 54(2): 177-182. https://doi.org/10.1016/S0167-7012(03)00037-X
[23] Padmavathy, N., Vijayaraghavan, R. (2011). Interaction of ZnO nanoparticles with microbes—A physio and biochemical assay. Journal of Biomedical Nanotechnology, 7(6): 813-822. https://doi.org/10.1166/jbn.2011.1343
[24] Zhang, L., Jiang, Y., Ding, Y., Povey, M., York, D. (2007). Investigation into the antibacterial behaviour of suspensions of ZnO nanoparticles (ZnO nanofluids). Journal of Nanoparticle Research, 9(3): 479-489. https://doi.org/10.1007/s11051-006-9150-1
[25] Sharma, D., Rajput, J., Kaith, B. S., Kaur, M., Sharma, S. (2010). Synthesis of ZnO nanoparticles and study of their antibacterial and antifungal properties. Thin Solid Films, 519(3): 1224-1229. https://doi.org/10.1016/j.tsf.2010.08.073
[26] Kadhim, R.G., Hussein, A.S. (2016). Study of optical properties of (PEO-PEG) blends. Journal of University of Kerbala, 14(4): 163-174.
[27] Hadi, A., Hashim, A., Al-Khafaji, Y. (2020). Structural, optical and electrical properties of PVA/PEO/SnO_2 new nanocomposites for flexible devices. Transactions on Electrical and Electronic Materials, 21(3): 283-292. https://doi.org/10.1007/s42341-020-00189-w
[28] Abdali, K., Abass, K.H., Al-Bermany, E., Al-Robayi, E. M., Kadim, A.M. (2022). Morphological, optical, electrical characterizations and anti-Escherichia coli bacterial efficiency (AECBE) of PVA/PAAm/PEO polymer blend doped with silver NPs. Nano Biomedicine and Engineering, 14(2): 114-122. https://doi.org/10.5101/nbe.v14i2.p114-122
[29] Alshiaa, S.A.O., Aziz, A.H.A., Zgair, I.A., Hasan, N.B. (2024). Impact of $CuCl_2$ addition to PMMA polymer on structural and optical properties. Revue des Composites et des Matériaux Avancés, 34(2): 189-194. https://doi.org/10.18280/rcma.340208
[30] Abdul Jabbar, G.A.H., Saeed, A.A., Al-Kadhemy, M.F.H. (2023). Optical characteristics and antibacterial activity of PVA/ZnO nanocomposites. International Journal of Nanoelectronics and Materials, 16(2): 431-440.
[31] Amin, K.M., Partila, A.M., Abd El-Rehim, H.A., Deghiedy, N.M. (2020). Antimicrobial ZnO nanoparticle–doped polyvinyl alcohol/pluronic blends as active food packaging films. Particle & Particle Systems Characterization, 37(4): 2000006. https://doi.org/10.1002/ppsc.202000006
[32] Kanmani, P., Rhim, J.W. (2014). Antimicrobial and physical-mechanical properties of agar-based films incorporated with grapefruit seed extract. Carbohydrate Polymers, 102(1): 708-716. https://doi.org/10.1016/j.carbpol.2013.10.099
[33] Khudair, I.A.H., AL-Shiaa, S.A.O., Al-Khaykanee, M.K. (2024). Enhancing the structural and optical properties of poly (vinyl alcohol) films through the incorporation of Ag2O: ZnO nanoparticle. Revue des Composites et des Matériaux Avancés, 34(3): 349-355. https://doi.org/10.18280/rcma.340310

NOMENCLATURE

A	Area
t	Time
k	Extinction of absorption
B	Material-dependent constant
υ	Frequency of the photon
Eg^{opt}	Optical bandgap energy
Eph	Phonon energy
h	Planck's constant
GS	Grain size

Greek symbols

α	Absorption coefficient
λ	Wavelength
β FWHM	Full width at half maximum (FWHM) of a peak in spectral analysis
$\cos\theta$	Part of diffraction or scattering equations